JOURNAL OF GEOPHYSICAL RESEARCH, VOL. 95, NO. B4, PAGES 4501–4510, APRIL 10, 1990

# Compaction and Inclination Shallowing in Deep-Sea Sediments From the Pacific Ocean

PORDUR ARASON AND SHAUL LEVI

*Geophysics, College of Oceanography, Oregon State University, Corvallis*

Progressive downcore shallowing of the remanent inclination has been observed in a 120-m section of marine sediments at Deep Sea Drilling Project site 578 in the northwest Pacific, representing the past 6.5 m.y. Near the top of the section the average inclination corresponds to the expected geocentric axial dipole value of 53° but shallows down section by about 6° to 8°. Northward translation of the Pacific plate accounts for only about a quarter of the inclination shallowing. Moreover, no inclination shallowing was observed at neighboring site 576, which has considerably lower sedimentation rates, and the last 5 m.y. are represented by a 26-m sedimentary section. We correlate the inclination shallowing at site 578 with an average decrease in porosity of 3–4%. The porosities in the top 26 m at site 576 are slightly higher than at site 578 and show no definite trend downhole. We interpret these results to suggest that both the downhole inclination shallowing and decrease of porosity in site 578 are caused by sediment compaction. Compaction does not play a significant role for the section at site 576 due to its much shorter length.

## INTRODUCTION

Paleomagnetism depends on accurate recording of the ancient geomagnetic field and the preservation of the magnetic remanence in the host rock. Many sediments have been shown to accurately preserve the paleomagnetic field direction; natural marine sediments often show no significant deviation from the expected geocentric axial dipole (GAD) inclination [e.g., *Harrison*, 1966; *Opdyke*, 1972; *Levi and Karlin*, 1989]. However, for some longer Deep Sea Drilling Project (DSDP) sedimentary sections, it was noticed that the inclinations at depth are shallower than expected, after correcting for tectonic movements, and these inclination anomalies have been qualitatively attributed to sediment compaction [e.g., *Morgan*, 1979; *Kent and Spariosu*, 1982; *Tauxe et al.*, 1984]. In these examples the postulated causal effects of compaction on the inclination shallowing have not been substantiated by independent quantitative methods. Inclination shallowing was associated quantitatively with sediment porosity in clays from the northwest Pacific Ocean [*Arason and Levi*, 1986], and *Celaya and Clement* [1988] reported correlations of inclination shallowing with dewatering in several cores from the Atlantic Ocean, where the carbonate contents are consistently greater than 80%. Laboratory studies have shown that compaction can contribute to inclination shallowing in sediments [e.g., *Blow and Hamilton*, 1978; *Anson and Kodama*, 1987]. In addition, *Arason and Levi* [this issue] have shown theoretically that a variety of mechanical models can produce inclination shallowing during compaction; the magnitude of the inclination shallowing may depend on factors such as the sediment lithology and the dominant physical processes responsible for the shallowing.

As sediments are buried they experience the overburden pressure from the accumulating sediment, which expels pore water and decreases the porosity [*Hamilton*, 1959, 1976]. The decrease of porosity can be used as a first-order estimate of sediment compaction. *Nobes et al.* [1986] examined the physical properties, including porosity, of clay rich sediments from all oceans for DSDP legs 1 to 86. This data set shows that in clayey deep-sea sediments the porosity changes downhole, from a 50–90% range in the top of the holes, to 40–80% at about 200 m below the seafloor, and to 30–50% near 1000 m depths. From their data we estimate the porosity gradients to range on average from 0.02 to 0.08% $m^{-1}$ in the top several hundred meters. Furthermore, these global porosity data suggest that sediment compaction in the top 100 m is a common property of marine sediments. Therefore, if sediment compaction can cause inclination shallowing, then slight inclination shallowing might be a common property of deep-sea sediments.

In this study we present paleomagnetic results from two DSDP sites. Interpretation of the magnetostratigraphy was straightforward due to the slowly changing sedimentation rates and excellent grouping of inclinations into antipodal polarities. The two sedimentary sections represent similar time intervals but different depths due to different sedimentation rates (site 578: 6.5 Ma in 120 m, and site 576: 5 Ma in 26 m). Although the inclinations near the top of both sections are close to the GAD value, the two sites do not show the same inclination changes back in time. We therefore conclude that the downhole inclination trends at site 578 are probably not of geomagnetic origin. Although it is possible that lithological variability of the sediment, coring disturbance, and even nonvertical drilling contributed to the downhole inclination patterns, we correlate the inclination shallowing in site 578 to the parallel downhole decrease in sediment porosity and suggest that compaction of the sediment caused rearrangement of grains leading to the observed inclination shallowing.

## DATA FROM PACIFIC OCEAN SEDIMENTS

In this study we consider results from DSDP sites 578 and 576 in the northwest Pacific Ocean (see Figure 1), cored in 1982 during leg 86 by the *D/V Glomar Challenger*. About 1000 km east of Japan (33.9°N, 151.6°E and 6010 m water depth) the hydraulic piston corer (HPC) was used to core a 177-m sedimentary section at site 578 with 99% recovery in the top 120 m. At site 576 (32.4°N, 164.3°E and 6217 m water depth) approximately 1200 km east of site 578, up to 75 m were cored in three holes using the HPC [*Heath et al.*, 1985*a*].

The top 120 m (~6.5 Ma) at site 578 consist of biosiliceous clay with locally abundant radiolarian-diatom ooze and numerous ash layers. This top section is comprised of two units; the upper



Paper number 89JB03584.
0148-0227/90/89JB-03584$05.00

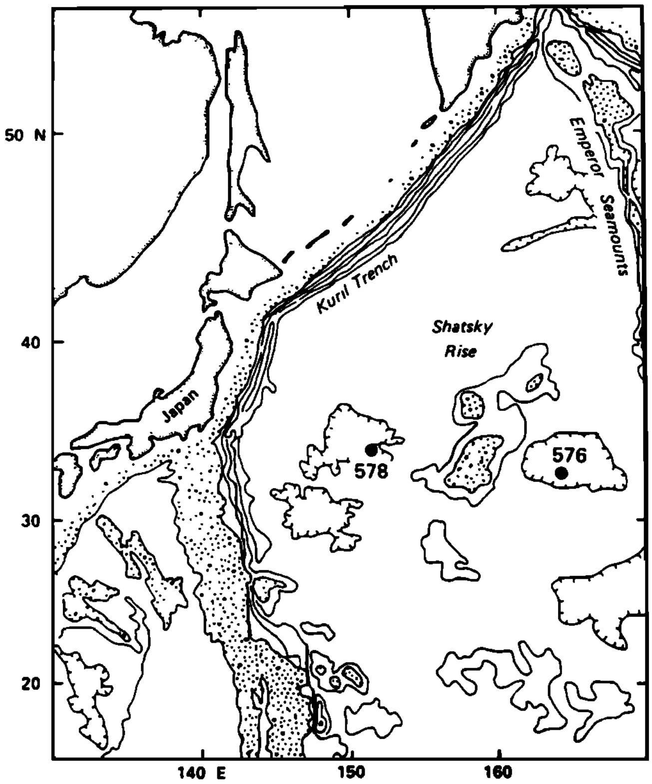


Fig. 1. Location map of DSDP sites 578 and 576 (modified from *Heath et al.* [1985*a*]).

77-m-thick unit is composed of gray anoxic clay which overlies a yellow-brown oxidized pelagic clay. The clay mineralogy of the sediment is approximately constant in the top 120 m, and the major clay minerals are 30% illite and 30% smectite. Below 120 m depth the mineralogy changes to 10% illite and 80% smectite and is more variable [*Lenôtre et al.*, 1985]. The sedimentation rate changes smoothly from about 10 m m.y.$^{-1}$ at 120 m depth, to 40 m m.y.$^{-1}$ near the top of the section. There are virtually no carbonates in the sediments at site 578 (less than 0.5% $CaCO_3$ [*Ku et al.*, 1985]). The top 27 m (~5 Ma) at site 576 consist of pelagic yellowish-brown, visibly burrowed, and slightly biosiliceous clay. The major clay minerals are approximately 30% illite and 30% smectite [*Lenôtre et al.*, 1985]. The sedimentation rate increases from about 2 m m.y.$^{-1}$ at 26 m depth, to 10 m m.y.$^{-1}$ near the top.

Samples for paleomagnetism were obtained during the cruise (approximately every 0.2 m at site 578, and 0.1 m at site 576) using a thin-walled, nonmagnetic stainless steel tube mounted in an oriented jig. The sediment was extruded from the 2 × 2 cm cross section sampling tube with a tightly fitting plastic piston into 8 cm$^3$ plastic sample boxes with lids. The samples were stored moist and at a temperature between 1° and 4°C. The intensities of the natural remanent magnetization (NRM) averaged about 50 mA m$^{-1}$ at site 578 and 20 mA m$^{-1}$ at site 576. The remanence directions are very stable, and minor secondary components were usually cleaned with 10 mT alternating field demagnetization (AFD), and the median demagnetizing fields of the NRM were about 30 mT. The remanence of all the paleomagnetic samples from site 576 (holes 576 and 576B) was measured, and they were demagnetized to at least 20 mT AFD [*Heath et al.*, 1985*b*]. Anomalous and pilot samples were taken to higher AFD levels. The subbottom depths for site 576 were adjusted according to correlations between the three holes by *Heath et al.* [1985*c*]. At site 578, initial measurements of the NRM and AFD to 10 mT were done for alternate samples [*Heath et al.*, 1985*b*]. Subsequently, we measured the remaining specimens in the top 120 m from site 578, which were demagnetized to at least 20 mT. No differences were observed between these two data sets for site 578.

Due to the excellent quality of the magnetic signal at site 578 and relatively rapid sedimentation rates, polarity magnetostratigraphy was possible down to 145 m subbottom, corresponding to about 15 Ma, but the quality of the magnetic signal deteriorates abruptly below 120 m depth (~6.5 Ma) which coincides with significant change in sedimentation rate and mineralogy. For these reasons we limit the discussion in this study to the top 13 cores (119 m) of site 578. At site 576, magnetostratigraphy was only possible down to 26 m (~5 Ma). Below this depth there is a sudden change in lithology and a sharp decrease in sedimentation rate. The magnetostratigraphy at these two sites is shown in Figure 2. In Figure 3 we show vector projections of the remanence during AFD of selected pilot samples from sites 578 and 576. The demagnetization trajectories show a linear decay to the origin with no major secondary components. A minor normal overprint was observed in the reversed samples where the AFD of 10 mT removed usually only a minute net magnetization. Most samples showed no directional change after 10 mT AFD. Based on the relatively high intensities of the NRM and anhysteretic remanent magnetization (ARM) and their demagnetization characteristics, we presume that the remanence is carried predominantly by submicron magnetite particles.

Part of the observed inclination shallowing at site 578 can be explained by the northward translation component of the Pacific plate. If the observed inclination shallowing at site 578 were entirely due to northward displacement through time (using the magnetic polarity timescale [e.g, *Ness et al.*, 1980] to transform depths to time), a northward component of motion of 121 ± 28 km m.y.$^{-1}$ would be required. The uncertainty represents the 95% confidence limit of the slope of a least squares line ($N = 563$). *Duncan and Clague* [1985] estimated a Pacific plate Euler rotation pole at 68.0°N, 75.0°W and rotation rate of 0.95° m.y.$^{-1}$ since 42 Ma, using K-Ar dating of nine linear island and seamount chains on the Pacific plate. This result causes a 30 km m.y.$^{-1}$ northward velocity component at site 578, and 35 km m.y.$^{-1}$ at site 576. Several estimates have been made of Pacific plate motion, with slightly different rotations, indicating about 10 km m.y.$^{-1}$ uncertainty in the northward velocity components at these sites. Therefore it seems that only about 25% of the observed inclination shallowing at site 578 can be explained by Pacific plate motion.

Following the magnetic measurements, most of the samples were used in detailed geochemical studies. One of the estimated parameters was the water content ($w$), from $w = ( m_w - m_d ) / m_d$; $m_w$ and $m_d$ are the weights of the wet and dried sediment, respectively. We determined the porosity ($\phi$) from the published water content data of *Heath et al.* [1985*c*], which we corrected for the salt content, using the relation

$$\phi = \frac{w}{w(1 - Sr) + r(1 - S)} \tag{1}$$

We assume sea water salinity, $S = 0.035$, and the ratio of the sea water density to the density of the sediment grains, $r = 1024/2700$.

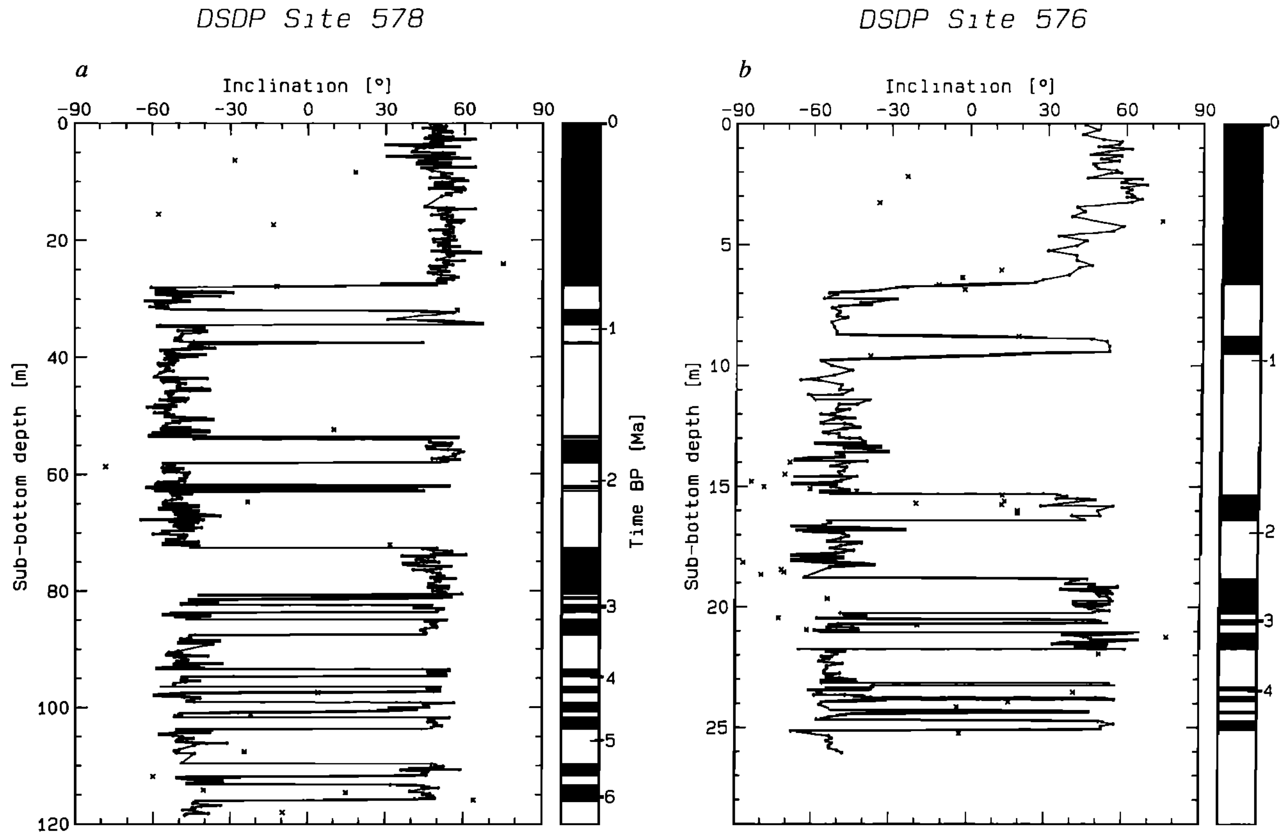


Fig. 2. Magnetostratigraphy at sites 578 and 576. The crosses represent excursional or transitional directions which were excluded from this study. (*a*) The inclination profile of the upper 120 m of hole 578, representing the most recent 6.5 m.y., showing all the recognized subchrons in this time-interval. (*b*) A composite section of inclinations in the top 26 m of holes 576 and 576B, representing the last 5 m.y. The downhole shallowing of the inclinations is visible in site 578, but there is no obvious trend at site 576.

## DATA ANALYSIS

### *Paleomagnetic Data Selection*

To focus on trends in the remanence, we analyzed the average behavior of the paleomagnetic directions. To be conservative, samples with excursion or transitional directions were omitted. Accordingly, using inclination and core-adjusted declination, we excluded specimens deviating from the GAD direction by more than 45°, as well as samples whose virtual geomagnetic pole latitudes deviated from the rotation axis by more than 20°, based only on the inclination data.

Of the 583 demagnetized specimens in the top 120 m of site 578, 20 were excluded from this study. Fourteen specimens were excluded because they deviated from the GAD direction by more than 45°, including eight excursions, five transitions, and one due to possible core top disturbance. An additional six samples were excluded because their virtual geomagnetic pole latitudes deviated from the rotation axis by more than 20°. These included two specimens with steep inclinations and four with shallow inclinations. Of the 328 demagnetized specimens in the top 26 m at site 576, 36 were excluded from this study. We omitted 16 specimens deviating from the GAD direction by more than 45°, including nine excursions, six transitions, and one possible core top disturbance. An additional 20 samples were excluded because their virtual geomagnetic pole latitudes deviated from the rotation axis by more than 20°. These included nine specimens with steep inclinations and 11 with shallow inclinations. To assess the influence of our data selection on the results, we repeated the analysis with all the data included.

### *Analysis of the Average Inclinations*

The selected "cleaned" inclination data (563 specimens from site 578 and 292 from site 576) are shown in Figure 4, transformed to positive inclinations. At site 578, there is a trend of downhole inclination shallowing of 6° to 8°, and a scatter of 10° to 15°. At site 576 we observe a slight but not significant inclination steepening trend of 1° to 2° and more scatter than at site 578. Since we are interested in the long-term trend, it is helpful to get rid of the high-frequency scatter, and this can be accomplished by averaging the inclinations over some depth or time interval. As these cores are azimuthally unoriented, the arithmetic means of the inclinations will have a bias, toward shallower inclinations. Therefore we used the method of *Briden and Ward* [1966] with formulas derived by *Kono* [1980]. A square averaging window was used, because it is directly applicable to the Kono equations, whereas weighting functions, such as the Gaussian, cannot be so readily used in the equations. Of some concern is the sharpness of the boxcar window, which produces some high-frequency noise. The averaging window was varied for optimum results; a too narrow window increased the 95% confidence limits, so that the changes downhole were not significant, and too wide windows smoothed out all variability.

First, we compare the inclinations at these two sites in time domain to study possible time related geomagnetic expressions.

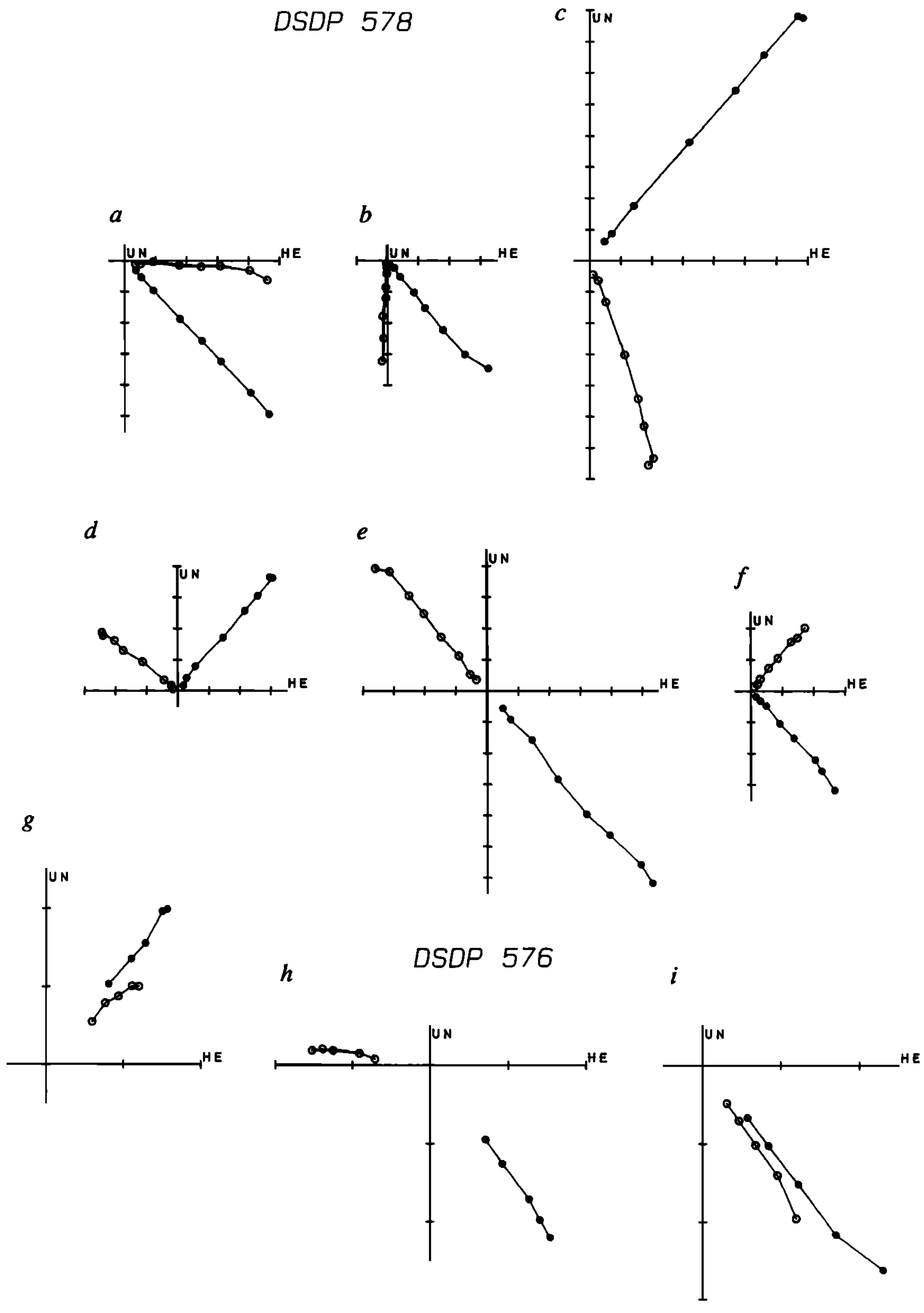


Fig. 3. Vector projections of selected pilot samples from sites 578 and 576. The ticks on the axes indicate 10 mA m$^{-1}$. Solid symbols show the inclination during demagnetization in an up (U) versus horizontal (H) projection, whereas open symbols show the relative declination during demagnetization in an north (N) versus east (E) projection. (*a*) – (*f*) Samples from site 578; NRM and demagnetization levels 10, 20, 30, 40, 60, 80, and 100 mT. (*a*) Sample 912 (578-1-2, 66) (hole-core-section, depth in section in centimeters) at 2.16 m depth below the seafloor. (*b*) Sample 946 (578-2-3, 128) at 9.06 m depth. (*c*) Sample 1074 (578-5-3, 26) at 36.56 m depth. (*d*) Sample 1198 (578-7-6, 106) at 60.76 m depth. (*e*) Sample 1290 (578-9-5, 83) 78.13 m depth. (*f*) Sample 1385 (578-11-5, 97) at 97.27 m depth. (*g*) – (*i*) Samples from site 576; NRM and demagnetization levels 10, 20, 30, and 40 mT. (*g*) Sample 36 (576-2-1, 96) at 7.91 m depth. (*h*) Sample 49 (576-2-2, 76) at 9.21 m depth. (*i*) Sample 192 (576-4-1, 106) at 19.96 m depth. The magnetization is very stable with only minor secondary components "cleaned" at the lowest demagnetization levels. The effect of minor overprinting are most noticeable in the reversed samples (Figures 3*c*, 3*d*, and 3*g*) where the demagnetization at 10 mT AFD removes only a minute net component.

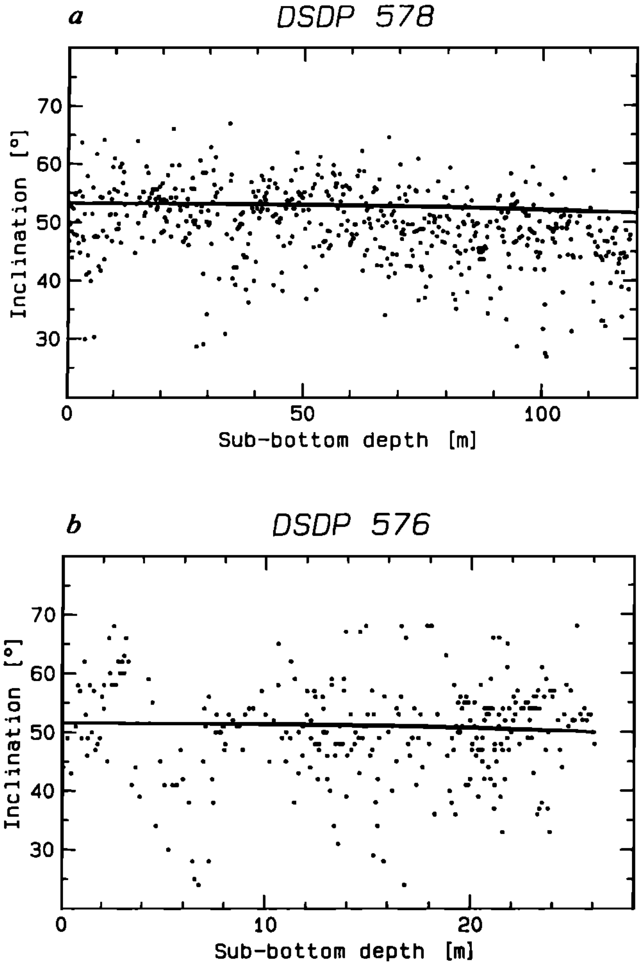


Fig. 4. The absolute values of the stable "cleaned" inclinations of the selected specimens used in this study. The curve on the graphs represents the geocentric axial dipole inclination of the sites with time transformed to depth. (*a*) The inclinations at site 578 show a definite trend with depth. The northward movement of the Pacific plate is not sufficient to account for the observed inclination shallowing with depth. (*b*) The inclinations at site 576 are more scattered, but there is no trend downcore.

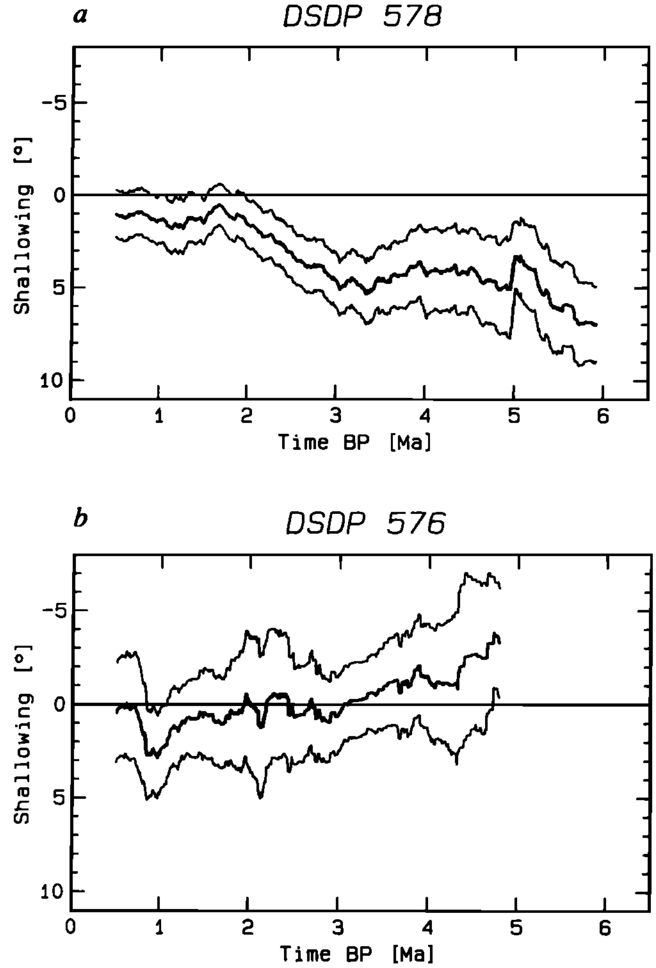


Fig. 5. A running 1-m.y. average of the inclination data back in time. The averages, shown by the bold curve, were calculated by the method of *Briden and Ward* [1966] and *Kono* [1980]. The average inclinations are shown as inclination shallowing, compared to the GAD value, corrected for the northward movement of the Pacific plate. The envelopes around the averages represent 95% confidence limits of the means ($\alpha_{95}$). (*a*) The inclinations at site 578 appear to have been much shallower than GAD prior to 2.5 Ma. (*b*) The running inclination averages for site 576 do not show shallowing back in time; rather they indicate a slight steepening.

Later in this paper we compare the inclinations in depth domain. The Briden and Ward/Kono average inclinations, as well as several Fisher statistics parameters, including 95% confidence limits of the mean, were calculated in the time domain with a 1-m.y. running boxcar. The inclination shallowing, after correcting for the northward motion of the Pacific plate (30 km m.y.$^{-1}$ for site 578, and 35 km m.y.$^{-1}$ for site 576) is shown in Figure 5. The running averages were also calculated without excluding the anomalous directions with no significant changes in the average values, but there was a slight increase in the 95% confidence limits of the means.

Figure 5 shows the different downcore behavior of the average inclinations for sites 578 and 576 over a comparable time interval. In addition, *Bleil* [1985] studied the paleomagnetism of site 579 (38.6°N, 153.8°E), also situated on the Pacific plate, about 560 km north of site 578. The sediments at site 579 were deposited since 4.5 Ma, and the trend of the site 579 inclinations is very similar to that at site 576, showing slight but not significant steepening. Therefore the inclination shallowing at site 578 is unlikely to be of geomagnetic origin, and we are led to conclude that the inclination shallowing at site 578 is caused by a recording or preservation problem in the sediment. The running averages were therefore also calculated in depth domain. We chose a 10-m window width for site 578 and a 5-m window for site 576. To study possible effects of compaction on the remanent inclination, we examined changes in physical properties downhole particularly the sediment porosity.

*Porosity Data*

In analyzing the porosity data we omitted samples associated with ash layers, because they often show a very distinct porosity signature. Of 311 porosity determinations at site 578, five samples were excluded, and at site 576 we excluded three samples out of 480. The mean porosity at site 578 is 79% and 82% at site 576. The selected porosity data (306 specimens for site 578 and 477 specimens for site 576) are shown in Figure 6. The data from site 578 indicate a porosity decrease of about 3–4% in the top 120 m, which is similar to the general trend of 0.02–0.08% m$^{-1}$ in clay-rich sediments of DSDP legs 1 to 86. *Schultheiss* [1985] conducted consolidation experiments with a few samples from sites 578 and 576. From these data [*Schultheiss*, 1985, Figures 9 and 12] we can estimate that a sample with 80% initial porosity will experience a porosity decrease of 0.03–0.07% m$^{-1}$ at 50–100 m depth, similar to the trend observed at site 578, suggesting that the

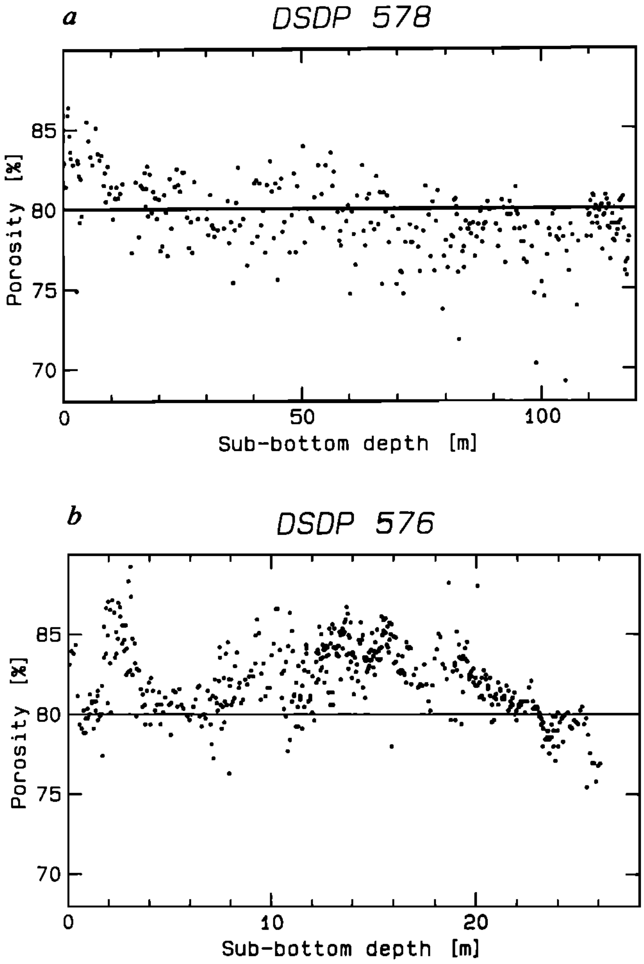


Fig. 6. The porosity of the sediments, calculated from drying individual samples. The horizontal line at 80% porosity was chosen arbitrarily for reference. (*a*) The porosities at site 578 show a definite downhole trend, which we interpret as dewatering due to gravitational compaction of the sediment. (*b*) The porosities at site 576 show no downhole trend mainly because of the difference of the depth scales. Note that site 576 has a higher mean porosity (i.e., is wetter) than site 578.

observed porosity decrease is a good indicator of compaction. The porosity data from site 576 do not show simple downhole behavior that can be readily interpreted as compaction; after a sharp fluctuation in the top 5 m the porosity increases downhole to about 15 m depth followed by a gradual decrease. Indeed, if site 576 had the same porosity trend as site 578 (0.03% $m^{-1}$), it would result in less than 1% change in this considerably shorter section (26 m), which would be close to our detection limit.

A simple running boxcar arithmetic average was used to smooth the variability in the porosity data and to calculate the 95% confidence limits of the means. The boxcar window was chosen for compatibility with the average inclination data, and its width was 10 m for site 578 and 5 m for site 576. The results are shown in Figure 7. The running averages were also analyzed when all the ash related porosities were included, and the results showed no noticeable changes.

## DISCUSSION

There is no apparent correlation between the magnetic and porosity data of individual specimens, which, we believe, is caused by high-frequency components in both signals, comparable or larger in amplitude than the trends (compare Figures 4 and 6 to Figure 7, noting that they show different scales). We have to average the direction over some time interval to decrease the effect of geomagnetic secular variation and other random noise in the magnetic signal. Similarly, the scatter in the individual porosity data also suggests that, strictly speaking, the initial porosity cannot be considered a constant through time. It may include high-frequency components in the initial porosity of the sediment, related to sedimentological variability due to climatic, lithologic, and provenance fluctuations. Therefore we have to integrate over these sediment fluctuations to be able to assume an on average constant initial porosity.

The running averages of the inclination shallowing and the porosity were calculated in depth domain and assigned the center depth of the running boxcar intervals (544 depths in site 578 centered from 5.0 to 113.6 m for 10-m windows at 0.2-m increments, and 212 depths in site 576 centered from 2.5 to 23.6 m using 5-m windows at 0.1-m increments). Note that these averages represent only a few independent estimates. The running averages of inclination shallowing and porosity for sites 578 and 576, together with 95% confidence limits, are shown in Figure 7. The depth domain running averages of the inclinations were plotted against the averages of the porosity in Figure 8, where it is seen that for site 578, inclination shallowing increases progressively with decreasing porosity, when the porosity decreases below about 80%. At site 576 the porosity is predominantly greater than 80%, and there is no significant shallowing or steepening of the inclinations (apart form core 1). In addition, Figure 8 also shows that the inclinations of the top cores (5–10 m) at sites 578 and 576 are anomalous, showing high scatter and some shallowing of the inclinations, not associated with downcore compaction. Coring disturbance seems to be common in the top core of DSDP hydraulic piston cores and may be related to a particular coring practice, where the first core is shot from above the sediment-water interface. Our suspicions might be supported by the considerable porosity fluctuation in the top cores, whose depth variation is repeated for all three holes at site 576. Therefore we suspect that the upper 5–10 m at sites 578 and 576 suffered subtle coring disturbance. It is unlikely that the inclination shallowing downhole can be adequately explained by nonvertical drilling with vertical penetration near the top and gradual bending to southerly 6°–8° off-vertical drilling. Although, downhole measurements of DSDP holes indicate that the drillstring can deviate up to 5° from the vertical, the within hole variation of this angle is considerably lower [*Wolejszo et al.*, 1974]. The oxidation change at 77 m depth at site 578 is of concern, because it occurs in the zone of strongest change in inclination shallowing between 60 m and 85 m. However, this oxidation boundary is not accompanied by change in clay mineralogy. In addition, Figure 9 shows that there are essentially no downhole changes in the magnetic properties, as suggested by the monotonous profiles of the NRM and ARM stability to alternating field demagnetization.

Tables 1 and 2 show the effect of polarity on the inclination shallowing. At first glance, the results of site 578 (Table 1) indicate that when the data are divided by chron, the reversed periods show more inclination shallowing than normal times. However, these differences are not significant at the 95% confidence levels. When all the data are considered together there is no significant difference in the inclination shallowing between normal and reversed polarity. For site 576 (Table 2) there is no significant inclination shallowing or steepening when the normal and reversed polarity data are divided by chron, or when all the normal and reversed data are pooled together. The present field inclination (IGRF 1985 [*Barker et al.*, 1986]) at sites 578 and 576 is about 8° shallower than the GAD value. Significant unidentified overprinting by the present field would cause normal

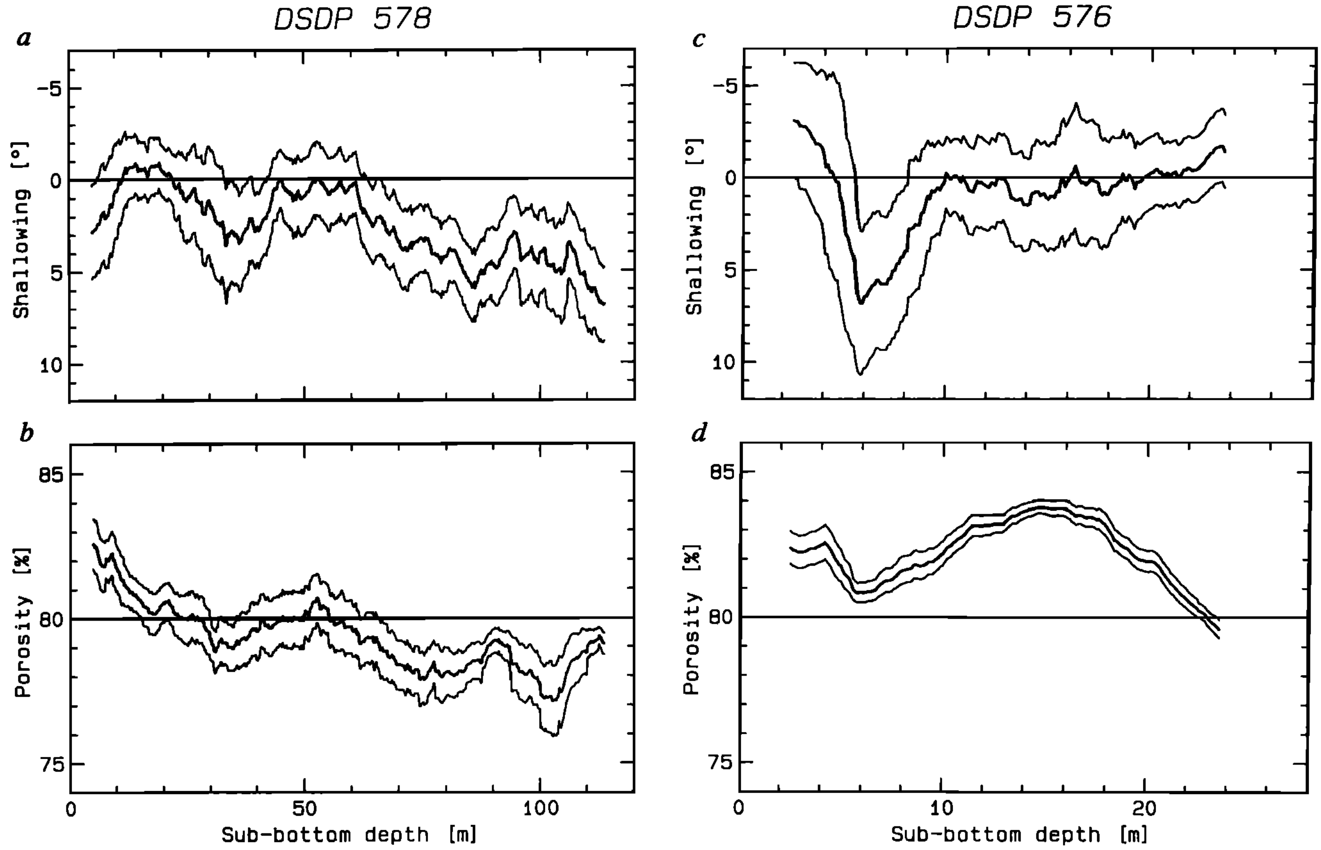


Fig. 7. A running average of the inclination and porosity data in depth domains. The shallowing was calculated with the same method as in Figure 5, with a fixed depth interval running window. The running averages are shown by a bold curve, enveloped by 95% confidence limits. (*a*) Average inclination shallowing at site 578. (*b*) Average porosities at site 578. The site 578 data were calculated every 0.2 m using a 10-m running window between 5.0 and 113.6 m (544 values). (*c*) Average inclination shallowing at site 576. (*d*) Average porosities at site 576. The site 576 averages were calculated every 0.1 m using a 5-m running window centered between 2.5 and 23.6 m (212 values). The downhole trends are now more visible than in Figures 4 and 6.

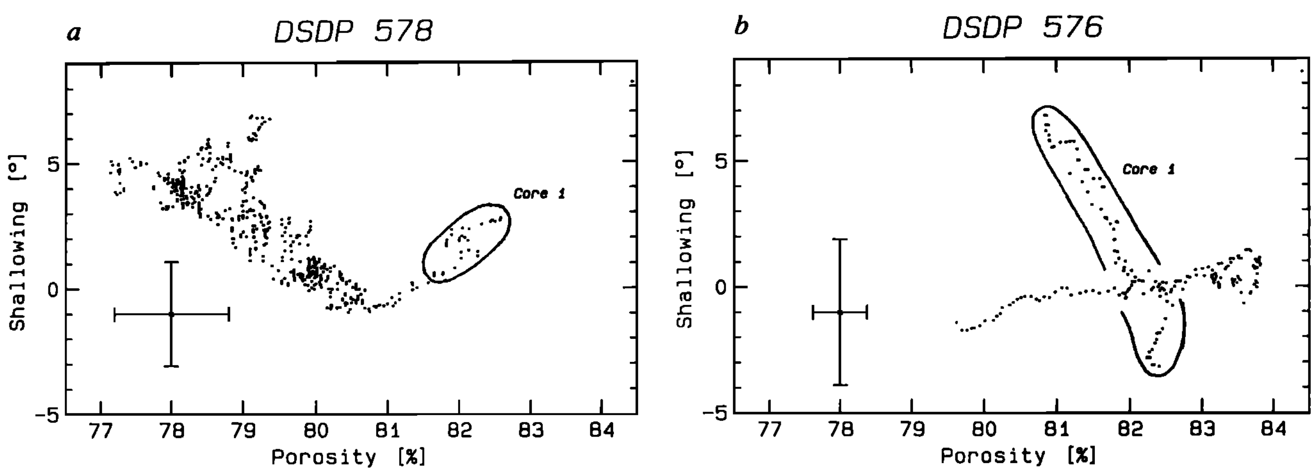


Fig. 8. Correlation between the running averages of the inclination shallowing and sediment porosity data (shown versus depth in Figure 7). The encircled tails are presumably disturbed data from the top core in each hole. The error bars represent the average 95% confidence limits from Figure 7. (*a*) Site 578: 10-m running averages (544 data) of inclination shallowing and porosity at identical depths. (*b*) Site 576: 5 m running averages (212 data) of inclination shallowing and porosity at identical depths. Apart from anomalous behavior in cores 1, site 576 shows no significant inclination shallowing or steepening.

zones to show inclination shallowing and reversed zones inclination steepening. Similarly, any biasing overprint during sampling and storage should affect normal and reversed samples in opposite directions. Since there is no systematic difference in the inclinations of normal and reversed samples, we can rule out problems due to possible unidentified overprinting.

Because of the proximity of sites 578 and 576 and their location on the same lithospheric plate, their different downcore inclination patterns cannot be caused by recent anomalous plate motions, true polar wander or long-term variations in the nondipole components of the Earth's magnetic field. Thus we interpret the results to indicate that the progressive inclination

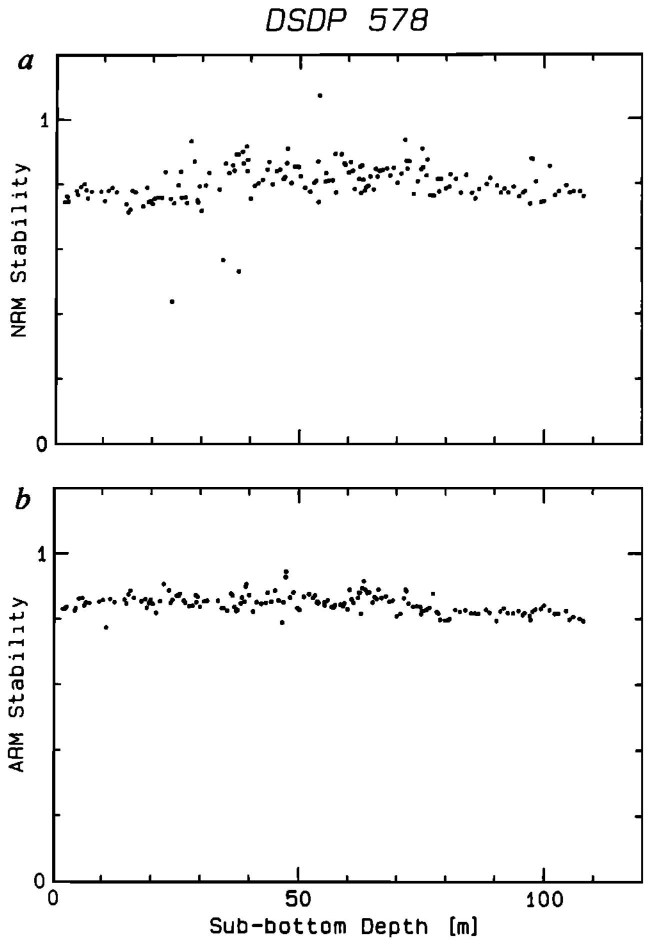


Fig. 9. Downhole stability of natural remanent magnetization (NRM) and anhysteretic remanent magnetization (ARM) of samples from site 578, as measured by the ratio $J_{20}/J_{10}$ of the intensity after 10 and 20 mT alternating field demagnetization (AFD). Of the 563 selected paleomagnetic samples used in this study we have measured ARM of 165. (*a*) Downhole NRM stability for the 165 samples for which ARM data is available. Most samples were cleaned at 10 mT. Note the small residual overprint at 10 mT, apparent in differences between polarities (higher and more dispersed for Matuyama 27.8–72.7 m). (*b*) Downhole stability of ARM. Note the similarity of the stability downhole, indicating the relative homogeneity of the magnetic properties.

shallowing at site 578 is caused by increasing compaction. Interestingly, there is no evidence for significant inclination shallowing in the top 50 m of site 578 or at site 576, where the porosities are generally greater than 80%. Hence there might be a threshold porosity for each sediment, which delineates the onset of inclination shallowing, which would be expected to be highly dependent on the sediment lithology.

The decrease in porosity, from an initial porosity $\phi_0$ to the porosity $\phi$, can be transformed to the normalized compaction values $\Delta V$ by the relation

$$\Delta V = \frac{\phi_0 - \phi}{1 - \phi} \tag{2}$$

The average porosity data from site 578 were transformed to compaction, using equation (2). The initial porosity was estimated to be 80.3% from Figure 8*a*. The results are shown in Figure 10, which excludes the data from disturbed core 1. In estimating the compaction we have assumed constant average

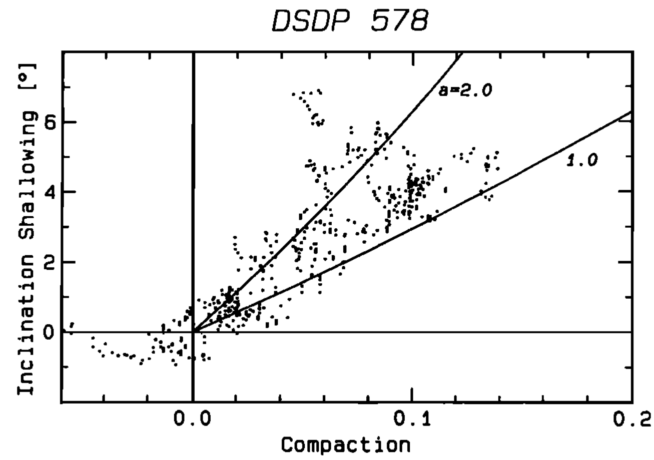


Fig. 10. Inclination shallowing versus sediment compaction at site 578. The data are the same as in Figure 8*a*, with porosities converted to compaction, assuming a constant initial porosity of 80.3%. The results of the disturbed core at the top of the hole are not shown. The data are compared to two values of the parameter *a* in equation (3); *a* = 1 and 2. The best fit in a least squares sense is *a* = 1.3.

initial porosity of the sediments. However, in the time interval represented by these sediments the sites had undergone long term sedimentation rate changes by a factor of four from the preglacial Pliocene to Pleistocene glaciations. In addition, slight variations in lithology may produce different initial sediment porosities. To investigate whether the onset of Pleistocene glaciations has significantly affected the porosity, we have compared the porosities of DSDP sites 576, 578, 579, and 580 (41.6°N, 154.0°E) in time domain but observed no consistent similarities that might be attributed to global climatic changes. Therefore we conclude that porosity changes can give a good first order estimate of sediment compaction, but further refinements may still be possible.

In Figure 10 we also show curves representing two values of the parameter *a* defined by the equation

$$\tan(I - \Delta I) = (1 - a\,\Delta V)\tan I \tag{3}$$

[*Arason and Levi*, this issue; *Anson and Kodama*, 1987] describing compaction produced inclination shallowing $\Delta I$, where $I$ is the inclination of the ambient field and $\Delta V$ is the compaction. For the results from site 578 the parameter *a* is between 1 and 2. In comparison, we estimated the parameter *a* to be about 4 for the inclination shallowing versus compaction for the carbonate-rich sediments studied by *Celaya and Clement* [1988]. Further studies are needed to determine if the parameter *a* has characteristic values for particular lithologies.

Paleomagnetists cannot generally use porosity as a check for compaction, because sufficient porosity data are usually unavailable for most cores and also because of the lack of successful theories and models to predict and subsequently correct the inclinations for compaction effects. However, the results of this study indicate that more careful attention must be paid to possible occurrences of inclination shallowing due to sediment compaction, and for the need to identify sediment lithologies and physical conditions which are likely to cause inclination anomalies. This, of course, has obvious implications for the use of inclination data from sediments for tectonic reconstructions and for studies of the long-term behavior of the geomagnetic field. In addition, there is a need for predictive models, that may eventually be used to correct for compaction produced inclination shallowing.

TABLE 1. Average Directions in DSDP Site 578

| Chron | Polarity | Depth Range, m | Number of Samples | Average Depth, m | Average Inclination, deg | Average GAD Inclination, deg | Inclination Shallowing, deg | $\alpha_{95}$, deg |
|---|---|---|---|---|---|---|---|---|
| Brunhes | N | 0.0–27.8 | 128 | 14.0 | 52.2 | 53.3 | 1.1 | 1.4 |
| Matuyama | N | 31.9–63.0 | 32 | 52.4 | 51.6 | 52.9 | 1.3 | 3.2 |
| | R | 27.8–72.7 | 186 | 50.6 | –51.2 | –52.9 | 1.7 | 1.2 |
| Gauss | N | 72.7–87.6 | 64 | 79.5 | 48.7 | 52.6 | 3.9 | 1.6 |
| | R | 80.7–85.0 | 14 | 83.1 | –45.2 | –52.5 | 7.3 | 4.1 |
| Gilbert | N | 93.5–103.7 | 28 | 99.0 | 48.1 | 52.1 | 4.0 | 3.4 |
| | R | 87.6–109.7 | 68 | 97.4 | –47.8 | –52.2 | 4.4 | 2.1 |
| Pre-Gilbert | N | 109.7–116.1 | 23 | 112.7 | 45.9 | 51.7 | 5.8 | 2.9 |
| | R | 111.8–118.6 | 20 | 115.7 | –43.2 | –51.6 | 8.4 | 3.0 |
| Selected | N | 0.0–116.1 | 275 | 50.6 | 50.4 | 52.8 | 2.4 | 1.0 |
| | R | 27.8–118.6 | 288 | 67.7 | –49.6 | –52.6 | 3.0 | 1.0 |
| | A | 0.0–118.6 | 563 | 59.4 | ±50.0 | ±52.7 | 2.7 | 0.7 |
| All | N | 0.0–116.1 | 283 | 51.0 | 50.5 | 52.8 | 2.3 | 1.3 |
| | R | 27.8–118.6 | 300 | 67.6 | –49.5 | –52.6 | 3.1 | 1.3 |
| | A | 0.0–118.6 | 583 | 59.6 | ±50.0 | ±52.7 | 2.7 | 0.9 |

The selected data are grouped by chrons and subchrons of normal (N) and reversed (R) polarity. Pre-Gilbert includes data between 5.41 and 6.42 Ma. The Selected normal and reversed data are grouped together, and also all absolute values (A). We also calculate the results for all samples (including transitions and excursions). Subbottom depth range of the samples is shown and the average of the sample depths in each group. Average inclinations were calculated using the method of *Briden and Ward* [1966], and *Kono* [1980], assuming the directions to be Fisherian [*Fisher*, 1953]. By assuming the poles to be Fisherian we get steeper average inclinations by 0.0°–0.2°. Average of the estimated geocentric axial dipole (GAD) inclinations were estimated assuming constant sedimentation rate between reversal boundaries, and 30 km m.y.$^{-1}$ northbound movement of site 578. The present location of Site 578 is 33.926°N, 151.629°E with GAD inclination of 53.4°. Inclination shallowing is the difference between average GAD inclination and the average of the observed inclinations. When the observed inclination is more horizontal than the GAD inclination, inclination shallowing is taken positive. Finally, the 95% confidence limits of the average inclination were estimated, and it is the same for the inclination shallowing since the GAD inclinations have very low uncertainty.

TABLE 2. Average Directions in DSDP Site 576

| Chron | Polarity | Depth Range, m | Number of Samples | Average Depth, m | Average Inclination, deg | Average GAD Inclination, deg | Inclination Shallowing, deg | $\alpha_{95}$, deg |
|---|---|---|---|---|---|---|---|---|
| Brunhes | N | 0.0–6.7 | 49 | 2.9 | 52.1 | 51.6 | –0.5 | 3.9 |
| Matuyama | N | 8.8–16.4 | 15 | 14.0 | 45.5 | 51.2 | 5.7 | 6.3 |
| | R | 6.7–18.8 | 107 | 12.8 | –51.1 | –51.2 | 0.1 | 2.1 |
| Gauss | N | 18.8–21.8 | 51 | 20.4 | 49.2 | 50.7 | 1.5 | 2.4 |
| | R | 20.3–21.1 | 13 | 20.7 | –50.6 | –50.7 | 0.1 | 4.4 |
| Gilbert | N | 23.2–25.1 | 9 | 24.2 | 53.1 | 50.2 | –2.9 | 3.0 |
| | R | 21.8–26.1 | 48 | 23.5 | –52.3 | –50.3 | –2.0 | 2.7 |
| Selected | N | 0.0–25.1 | 124 | 13.0 | 50.2 | 51.1 | 0.9 | 2.0 |
| | R | 6.7–26.1 | 168 | 16.5 | –51.4 | –50.9 | –0.5 | 1.6 |
| | A | 0.0–26.1 | 292 | 15.0 | ±50.9 | ±51.0 | 0.1 | 1.2 |
| All | N | 0.0–25.1 | 136 | 13.2 | 50.0 | 51.1 | 1.1 | 2.9 |
| | R | 6.7–26.1 | 192 | 16.3 | –53.3 | –50.9 | –2.4 | 2.7 |
| | A | 0.0–26.1 | 328 | 15.0 | ±51.9 | ±51.0 | –0.9 | 2.0 |

See Table 1 footnotes for description of individual columns. Negative inclination shallowing indicate steeper average inclinations than the GAD value. The present location of Site 576 is 32.356°N, 164.276°E with present GAD inclination of 51.7°. The northbound velocity of site 576 is assumed 35 km m.y.$^{-1}$.

*Acknowledgments.* We thank D. Schultz for assistance in the laboratory and R. B. Kovar and C. Lopez for supplying the geochemical data from DSDP leg 86 in digital form. Discussions with R. A. Duncan on Pacific plate motions are greatly appreciated. Two anonymous reviewers and an associate editor made constructive comments. This work was supported by the National Science Foundation and the Icelandic Government Student Loan Fund.

## REFERENCES

Anson, G. L., and K. P. Kodama, Compaction-induced shallowing of the post-depositional remanent magnetization in a synthetic sediment, *Geophys. J. R. Astron. Soc.*, *88*, 673-692, 1987.

Arason, P., and S. Levi, Inclination shallowing recorded in some deep sea sediments (abstract), *Eos Trans. AGU*, *67*, 916, 1986.

Arason, P., and S. Levi, Models of inclination shallowing during sediment compaction, *J. Geophys. Res.*, this issue.

Barker, F. S., et al., International geomagnetic reference field revision 1985, *Eos Trans. AGU*, *67*, 523-524, 1986.

Bleil, U., The magnetostratigraphy of northwest Pacific sediments, Deep Sea Drilling Project leg 86, *Initial Rep. Deep Sea Drill. Proj.*, *86*, 441-458, 1985.

Blow, R. A., and N. Hamilton, Effect of compaction on the acquisition of a detrital remanent magnetization in fine-grained sediments, *Geophys. J. R. Astron. Soc.*, *52*, 13-23, 1978.

Briden, J. C., and M. A. Ward, Analysis of magnetic inclination in borecores, *Pure Appl. Geophys.*, *63*, 133-152, 1966.

Celaya, M. A., and B. M. Clement, Inclination shallowing in deep sea sediments from the north Atlantic, *Geophys. Res. Lett.*, *15*, 52-55, 1988.

Duncan, R. A., and D. A. Clague, Pacific plate motion recorded by linear volcanic chains, in *The Ocean Basins and Margins*, vol. 7A, edited by A. E. M. Nairn, F. G. Stehli, and S. Uyeda, pp. 89-121, Plenum, New York, 1985.

Fisher, R., Dispersion on a sphere, *Proc. R. Soc. London, Ser. A*, *217*, 295-305, 1953.

Hamilton, E. L., Thickness and consolidation of deep-sea sediments, *Geol. Soc. Am. Bull.*, *70*, 1399-1424, 1959.

Hamilton, E. L., Variations of density and porosity with depth in deep-sea sediments, *J. Sediment Petrol.*, *46*, 280-300, 1976.

Harrison, C. G. A., Paleomagnetism of deep sea sediments, *J. Geophys. Res.*, *71*, 3035-3043, 1966.

Heath, G. R., et al., *Initial Reports of the Deep Sea Drilling Project*, *86*, 804 pp., U.S. Government Printing Office, Washington, D.C., 1985*a*.

Heath, G. R., D. H. Rea, and S. Levi, Paleomagnetism and accumulation rates of sediments at sites 576 and 578, Deep Sea Drilling Project leg 86, western north Pacific, *Initial Rep. Deep Sea Drill. Proj.*, *86*, 459-502, 1985*b*.

Heath, G. R., R. B. Kovar, C. Lopez, and G. L. Campi, Elemental composition of Cenozoic pelagic clays from deep sea drilling project sites 576 and 578, western north Pacific, *Initial Rep. Deep Sea Drill. Proj.*, *86*, 605-646, 1985*c*.

Kent, D. V., and D. J. Spariosu, Magnetostratigraphy of Caribbean site 502 hydraulic piston cores, *Initial Rep. Deep Sea Drill. Proj.*, *68*, 419-433, 1982.

Kono, M., Statistics of paleomagnetic inclination data, *J. Geophys. Res.*, *85*, 3878-3882, 1980.

Ku, T. L., J. R. Southon, J. S. Vogel, Z. C. Liang, M. Kusakabe, and D. E. Nelson, $^{10}$Be distributions in deep sea drilling project site 576 and site 578 sediments studied by accelerator mass spectrometry, *Initial Rep. Deep Sea Drill. Proj.*, *86*, 539-546, 1985.

Lenôtre, N., H. Chamley, and M. Hoffert, Clay stratigraphy at Deep Sea Drilling Project sites 576 and 578, leg 86 (western north Pacific), *Initial Rep. Deep Sea Drill. Proj.*, *86*, 571-579, 1985.

Levi, S., and R. Karlin, A sixty thousand year paleomagnetic record from Gulf of California sediments: Secular variation, late Quaternary excursions and geomagnetic implications, *Earth Planet. Sci. Lett.*, *92*, 219-233, 1989.

Morgan, G. E., Paleomagnetic results from DSDP site 398, *Initial Rep. Deep Sea Drill. Proj.*, *47*, 599-611, 1979.

Ness, G., S. Levi, and R. Couch, Marine magnetic anomaly timescales for the Cenozoic and Late Cretaceous: A précis, critique, and synthesis, *Rev. Geophys.*, *18*, 753-770, 1980.

Nobes, D. C., H. Villinger, E. E. Davis, and L. K. Law, Estimation of marine sediment bulk physical properties at depth from seafloor geophysical measurements, *J. Geophys. Res.*, *91*, 14,033-14,043, 1986.

Opdyke, N. D., Paleomagnetism of deep-sea cores, *Rev. Geophys.*, *10*, 213-249, 1972.

Schultheiss, P. J., Physical and geotechnical properties of sediments from the northwest Pacific: Deep Sea Drilling Project leg 86, *Initial Rep. Deep Sea Drill. Proj.*, *86*, 701-722, 1985.

Tauxe, L., P. Tucker, N. P. Petersen, and J. L. LaBrecque, Magnetostratigraphy of leg 73 sediments, *Initial Rep. Deep Sea Drill. Proj.*, *73*, 609-621, 1984.

Wolejszo, J., R. Schlich, and J. Segoufin, Paleomagnetic studies of basalt samples, Deep Sea Drilling Project, leg 25, *Initial Rep. Deep Sea Drill. Proj.*, *25*, 555-572, 1974.

P. Arason and S. Levi, Geophysics, College of Oceanography, Oregon State University, Oceanography Admin Bldg 104, Corvallis OR 97331-5503.

(Received March 2, 1989;
revised October 30, 1989;
accepted November 26, 1989.)